

Supporting Information:

**Ambient-Pressure Soft X-Ray Absorption
Spectroscopy of a Catalyst Surface in Action:
Closing the Pressure Gap in the Selective
n-Butane Oxidation over Vanadyl Pyrophosphate**

Christian Heine,[†] Michael Hävecker,^{†,‡} Eugen Stotz,[†] Frank Rosowski,^{¶,§} Axel Knop-Gericke,[†] Annette Trunschke,[†] Maik Eichelbaum,^{*,†,¶} and Robert Schlögl[†]

*Department of Inorganic Chemistry, Fritz-Haber-Institut der Max-Planck-Gesellschaft,
Faradayweg 4-6, 14195 Berlin, Germany, Solar Energy Research, Helmholtz-Zentrum
Berlin / BESSY II, Albert-Einstein-Straße 15, 12489 Berlin, Germany, BasCat, UniCat
BASF JointLab, TU Berlin, Marchstraße 6, 10587 Berlin, Germany, and Process Research
and Chemical Engineering, Heterogeneous Catalysis, BASF SE, Carl-Bosch-Straße 38,
67056 Ludwigshafen, Germany*

E-mail: me@fhi-berlin.mpg.de

Phone: +49 (0)30 84134566. Fax: +49 (0)30 84134401

*To whom correspondence should be addressed

[†]Fritz-Haber-Institut

[‡]Helmholtz-Zentrum Berlin

[¶]BasCat

[§]BASF SE

Variable-pressure NEXAFS setup

The experimental setup is shown in Figure S1. The variable-pressure NEXAFS system is divided in a low pressure, a reaction and an optic section. The low pressure section consists of a differential pumping stage (CF 63/40 cross) connected by a flexible CF 40 metal tube with an x-y stage for X-ray beam alignment. It is connected to the Bessy II ISIS beamline and separated by an X-ray transparent Si_3N_4 membrane from the reaction section. The X-ray membrane ($1.0 \times 1.0 \text{ mm}^2$, thickness: 150 nm) mounted into a $17.5 \times 17.5 \text{ mm}^2$, 200 μm thick wafer is glued with high temperature epoxy (EPO-TEK 353 ND) on a stainless steel tube. The epoxy has to seal the low pressure section and to resist the temperatures (400°C sample temperature) in front of the reaction cell. The distance between the X-ray membrane and the sample container (typically 2 mm) can be adjusted in order to minimize the X-ray path length while avoiding an overheating of the membrane. The stainless steel tube with the X-ray membrane is connected with a Swagelok ultra torr UHV fitting adapter to a CF 40 flange (Figure S1b). The X-ray membrane is specified to resist a pressure differential of 1000 mbar under static conditions. The low pressure section is slowly pumped to 1 mbar ($\Delta p/\Delta t \approx 0.3 \text{ mbar/s}$) by a diaphragm pump to achieve a quasi static force on the X-ray membrane. Afterwards the operation pressure of 10^{-7} mbar is reached with a turbo molecular pump.

The reaction and the optic section are mounted on a rack movable in the x, y and z direction and connected via a flexible CF 40 metal tube with the low pressure section. Thus, the alignment of the X-ray membrane is decoupled from the alignment of the X-ray beam. The reaction gas supply of the reaction chamber (CF 40 cube) is arranged by Bronkhorst mass flow controllers. For the supply and exhaust pipe system Swagelok VCR connectors are used. The exhaust pipe system is heated, preventing a condensation of reaction products. The reaction gas enters the reaction chamber via a CF 40/Swagelok adapter flange, flows through the central hole in the Faraday cup (diameter 1 mm) of the reaction cell, passes the sample pellet and leaves the reaction cell through a hole in its bottom pumped by the process pumps. Details about the reaction cell will be described in the respective section. A PID

controller (RVC 300 Pfeiffer Vacuum) keeps the desired pressure in the reaction chamber constant via a feedback loop between the throttle valve and the capacitance pressure gauge at the gas inlet of the reaction chamber. After the gas passes the throttle valve the process pumps control the pressure in front of the mass spectrometer (Pfeiffer Omnistar GSD320 VARI), which was kept constant during the experiment (5.5 mbar). The used system is a conventional quadrupol mass spectrometer with a heated inlet valve, that automatically adapts the gas flow into the mass spectrometer recipient to obtain a constant recipient pressure of 2×10^{-6} mbar.

A 808 nm, cw infrared (IR) laser (LIMO Lissotschenko Mikrooptik) is used to heat the sample. The laser beam is guided through a fiber optic cable into the beam shaping module. The beam has a quadratic shape ($5.0 \times 5.0 \text{ mm}^2$ at sample position) when leaving the module. It illuminates a steel plate at the backside of the sample pellet, thus heating the sample (cf. Figure S2). A PID feedback loop between a K-type thermocouple in front of the sample pellet and the laser source controls the sample temperature. The optical section is separated from the reaction section by a quartz window with anti-reflection coating optimized for 808 nm transmission.

Reaction cell

A schematic of the front and the cross section of the reaction cell, the sample carrier and the sample stage are shown in Figure S2. The sample pellet mounted on a steel plate is gripped in a groove of a ceramic (MACOR) mold body and fixed with a nut from the rear. The distance between the Faraday cup like lid of the sample container and the sample surface is $900 \mu\text{m}$ creating a reaction volume of roughly $20 \mu\text{l}$. A K-type thermocouple is fixed at the interface between the sample pellet and the ceramic mold body by a nut (Figure S2a). The Faraday cup is fixed with two plates in front of the sample pellet on the ceramic mold body, which is itself mounted on a sapphire sample carrier by four screws. Spring loaded bolts

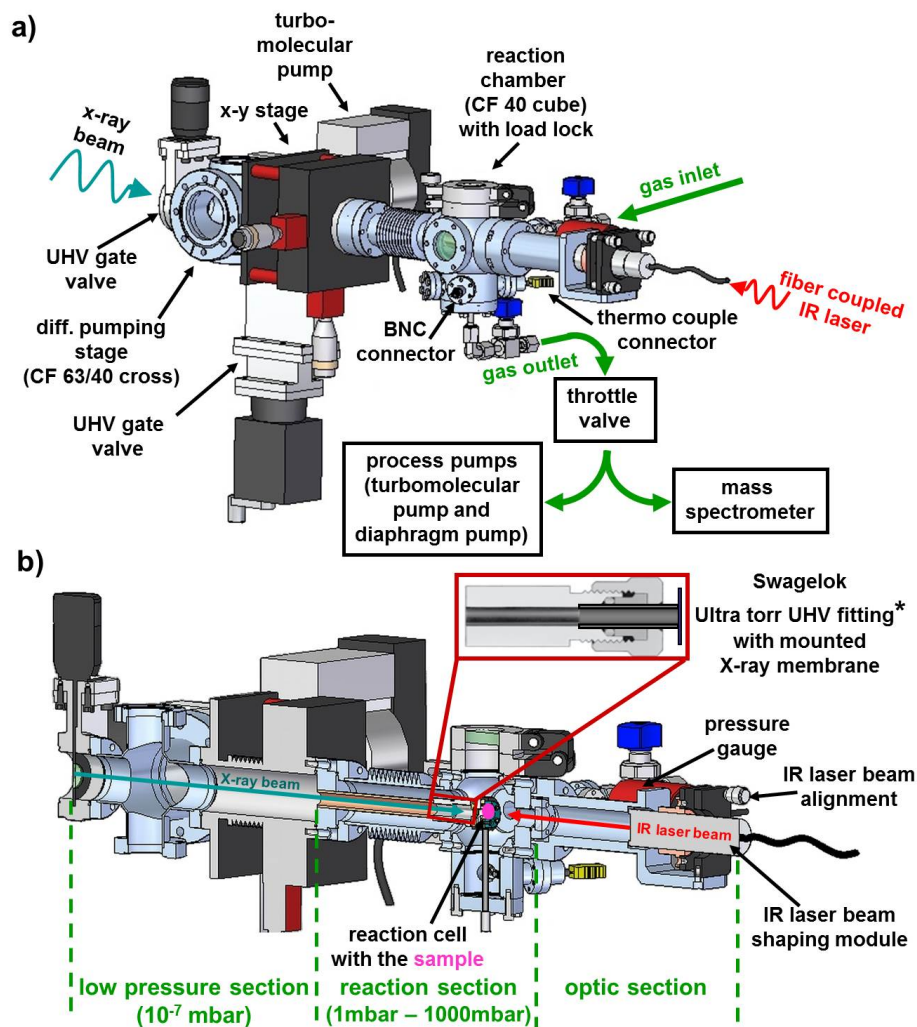


Figure S 1: Drawings of the high-pressure NEXAFS setup comprising the low pressure, reaction and optic section installed at the BESSY II ISISS beamline.

mounted in a MACOR body of the sample stage realise the electric contact to the screws mounted at the sapphire sample carrier and allow connection to vacuum feedthroughs via wires. Two of the screws are connecting the thermocouple to the PID thermocontroller. The third screw is electrically connected with the Faraday cup via a metal plate to apply a potential. The fourth screw is electrically insulated from the Faraday cup like lid via a ceramic (MACOR) to avoid any leak current (Figure S2b). The gas outlet at the sample stage is sealed to the reaction cell body via an O-ring. Thus, the complete reaction cell unit can easily be removed with the sapphire sample carrier from the sample stage for sample

exchange without disassembling any connections. The sapphire sample carrier and the IR laser heating are well proven concepts applied since a long time in the NAP-XPS setups of FHI.¹⁻³

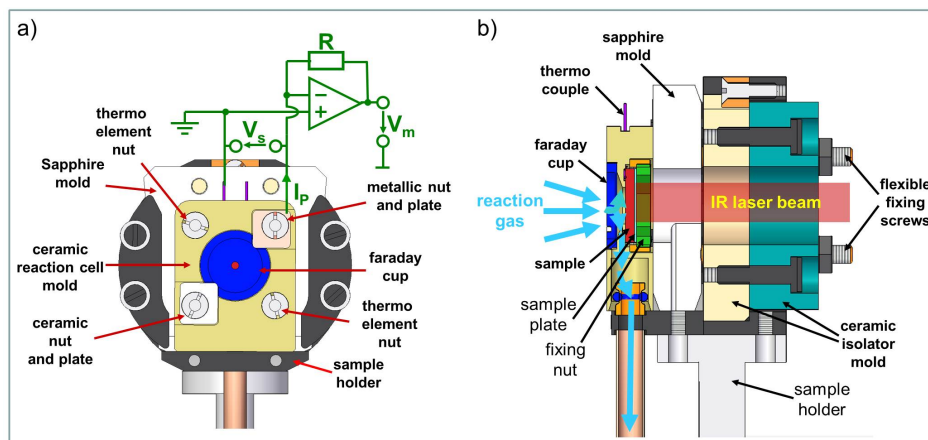


Figure S 2: Schematic of the front (a) and the cross section (b) of the reaction cell.

Measurement principle (photocurrent measurement)

The impinging X-ray photon beam generates an electron hole pair in the solid. In the case of the vanadium $L_{2,3}$ -edges transitions between occupied V 2p and unoccupied V 3d states take place. In the non-radiating decay process of the electron hole pair recombination, Auger-Meitner (AM) electrons are generated and mainly contribute to the total electron yield (TEY). Thus, the TEY mode is surface sensitive because the inelastic mean free path length of AM electrons is approximately 1 nm.⁴ In addition to the absorption in the solid also X-ray absorption in the gas phase occurs resulting in two methodological challenges. On the one hand the photon number reaching the sample position decreases strongly with increasing X-ray path length in the gas. This is exemplified in Figure S3 where the X-ray transmission in the photon energy range between 100 and 1000 eV is compared for a 10 mm path in air and 3 mm path in a butane/oxygen/helium reaction mixture. It becomes obvious that path lengths in the mm range are required for sufficient signal strength in the soft X-ray regime. The transmission of the X-ray membrane (150 nm Si_3N_4) used to seal the reaction

part from the vacuum part of the beamline is shown for comparison. On the other hand the absorbed X-rays in the gas phase ionize the gas molecules and create electron-ion pairs. Electrons created by this process are detected as well. Thus, the K-edge of gas phase oxygen in addition to the oxygen K-edge of VPP is visible in the spectra.

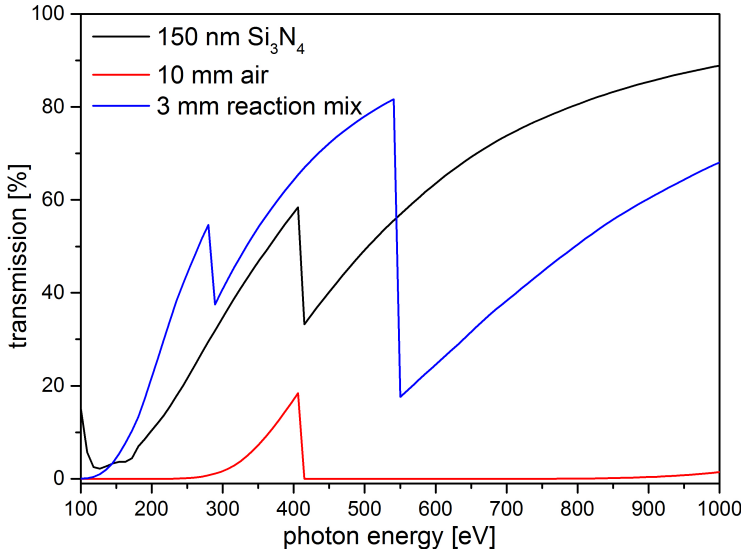


Figure S 3: X-ray transmission in a 10 mm path in air and 3 mm path in a n-butane/oxygen/helium reaction mixture (always at 1000 mbar), and, for comparison, transmission of the X-ray membrane (150 nm Si_3N_4) used to seal the reaction from the vacuum section of the beamline.

For the detection of photoelectrons, a voltage V_S is applied between the sample (grounded by the thermocouple) and the Faraday cup (+108 V) (Figure S2a). The by the absorption process generated primary Auger electrons and secondary electrons are moderately accelerated to the Faraday cup by the electric field and a photocurrent I_P is measured via a transimpedance amplifier (by measuring the voltage $V_A = -R$ (resistance) I_P). On their way to the Faraday cup the high kinetic Auger electrons ionize gas molecules and a cascade of secondary electrons ("environmental secondaries") is generated until their energy is below the threshold for gas ionization, additionally enhancing the TEY. The described measurement principle is called conversion electron yield mode (CEY). Only fast electrons are able to

ionize gas molecules. Thus, in contrast to the TEY mode where the spectrum is dominated by slow electrons, in the CEY mode the contribution of fast electrons to the spectrum might be enhanced.

NEXAFS experiments and data evaluation

In situ NEXAFS experiments were performed at the synchrotron radiation facility BESSY II in Berlin. The described instrument was connected to the ISIS (innovative station for in situ spectroscopy) beamline. The sample was probed with monochromatic light from 505 to 529 eV to investigate the vanadium L₂-, L₃- and oxygen K-edge. For the in situ NEXAFS experiments 10 mg of the VPP powder were pressed into a self-supporting pellet (1 ton pressing pressure, diameter of pellet: 8 mm). The sample pellet was heated to 400°C with a heating rate of 10 K/min in 1.5 % n-butane, 20 % oxygen and helium as balance at 3 mbar. Reference spectra were first taken at 3 mbar to test the CEY measurement and the stability of the X-ray membrane, which is not only strained by the pressure difference between the low pressure and reaction section, but also by the X-ray illumination and local heat transfer from the sample surface via the Faraday cup onto the membrane, in particular at higher pressures where heat conductivity via the gas becomes relevant. Afterwards the measurements at 10 mbar, 100 mbar and 1000 mbar were performed. The measurement protocol is shown in Table S1.

It is well known that the $1\sigma_u \rightarrow \pi^*$ transition of molecular oxygen at 531 eV can enormously affect the background of the vanadium L_{2,3}-edge spectra. In particular, the L₂-edge at 524 eV interferes heavily with the π^* resonance and the Coster-Kronig decay channel.⁵ Therefore, only the L₃-edges at 517.5 eV were evaluated. In order to correct the L₃-edge spectrum of VPP for the π^* resonance of molecular oxygen, a gold foil, which does not form an oxide layer under the applied conditions, was mounted on the sample holder to measure the K-edge of molecular oxygen at room temperature as reference spectrum. The oxidizing

Table S 1: Measurement protocol for the in situ NEXAFS measurement of VPP.

index	T [°C]	p [mbar]	gas composition [%]			period [h]
			n-butane	oxygen	helium	
1	400	10	1.5	20	78	1
2	400	100	1.5	20	78	1
3	400	1000	1.5	20	78	2
4	400	10	1.5	20	78	0.5
5	400	10	0	20	80	1
6	400	100	0	20	80	1
7	400	1000	0	20	80	1
8	400	10	1.5	0	98	1
9	400	100	1.5	0	98	1
10	400	1000	1.5	0	98	1

conditions (20% oxygen in He) were applied and spectra were taken from 505 to 560 eV between 3 and 1000 mbar. These reference measurements were used for background correction. In the case of the experiments at 10 and 100 mbar it turned out that a simple linear background subtraction at the vanadium L₃-edge is suitable. Spectra at 1000 mbar in the presence of oxygen were corrected by the subtraction of the appropriate oxygen reference spectrum. All spectra are the sum over 5 raw data sets. The photon energy scale is adjusted to the π^* resonance of gas phase oxygen at around 531 eV.

Microwave conductivity measurements

The microwave cavity perturbation setup used to measure the conductivity and the measurement protocol were described in detail previously.⁶ In short, as resonator a cylindrical X-band TM₁₁₀ silver-plated brass cavity (ZWG Berlin-Adlershof) with a height of 19.5 mm and a diameter of 38.5 mm was used. A quartz tube reactor with 4 mm outer and 3 mm inner diameter containing the sample under investigation (powders were filled in with a bed height of 10 mm and embedded within quartz wool) and surrounded by a 10 mm outer diameter double-walled quartz dewar mantle was directly placed in the center of the cavity. As for the 1000 mbar measurement, the quartz tube flow through reactor was connected upstream to a gas delivery manifold equipped with mass flow controllers (Bronkhorst El-Flow) to supply the different gas mixtures. For the 10 mbar dynamic vacuum measurement a quartz cell equipped with Teflon Duran valves was used which was connected to a vacuum system that allows the dosing of gases and the adjustment of the total pressure in the reactor cell. Heating of the reactor was performed by preheating a stream of 8 l/min N₂ in a resistive furnace consisting of a Sylvania tungsten series I heater. The cavity was connected to a vector network analyzer (Agilent PNA-L N5230C-225) in order to record resonance spectra of S₁₁-parameters in reflection mode (reflected power versus frequency) and to determine the resonance frequency and quality factor of the cavity with and without sample. The

microwave power attenuation was set to 11 dBm. From the change of the quality factor with and without sample Q_2 and Q_1 , respectively, the imaginary part of the permittivity ϵ_2 (after applying the Landau-Lifshitz-Looyenga effective medium theory to calculate the permittivity of the solid from the powder permittivity) and finally the conductivity σ were calculated after

$$B\epsilon_2 \frac{V_s}{V_c} = \left(\frac{1}{Q_2} - \frac{1}{Q_1} \right) \quad (1)$$

$$\sigma = \epsilon_0 \omega_2 \epsilon_2 \quad (2)$$

with B being the calibration factor of the cavity determined with reference samples, V_c the volume of the cavity, V_s the volume of the sample, ϵ_0 the vacuum permittivity and ω_2 the resonance frequency of the cavity with sample.

References

- (1) Hävecker, M.; Pinna, N.; Weiß, K.; Sack-Kongehl, H.; Jentoft, R. E.; Wang, D.; Swoboda, M.; Wild, U.; Niederberger, M.; Urban, J.; Su, D. S.; Schlögl, R. Synthesis and Functional Verification of the Unsupported Active Phase of VxOy Catalysts for Partial Oxidation of n-Butane. *J. Catal.* **2005**, *236*, 221–232.
- (2) Zemlyanov, D.; Aszalos-Kiss, B.; Kleimenov, E.; Teschner, D.; Zafeiratos, S.; Hävecker, M.; Knop-Gericke, A.; Schlögl, R.; Gabasch, H.; Unterberger, W.; Hayek, K.; Klötzer, B. In Situ XPS Study of Pd(1 1 1) Oxidation. Part 1: 2D Oxide Formation in 10^{-3} mbar O₂. *Surf. Sci.* **2006**, *600*, 983–994.
- (3) Rocha, T.; Oestereich, A.; Demidov, D. V.; Hävecker, M.; Zafeiratos, S.; Weinberg, G.; Bukhtiyarov, V.; A., K.-G.; Schlögl, R. The Silver-Oxygen System in Catalysis: New Insights by Near Ambient Pressure X-Ray Photoelectron Spectroscopy. *Phys. Chem. Chem. Phys.* **2012**, *14*, 4554–4564.

- (4) Tanuma, S.; Powell, C.; Penn, D. *Surf. Interf. Anal.* **1994**, *21*, 165–176.
- (5) Coster, D.; Kronig, R. D. L. New Type of Auger Effect and its Influence on the X-Ray Spectrum. *Physica* **1935**, *2*, 13 – 24.
- (6) Eichelbaum, M.; Stößer, R.; Karpov, A.; Dobner, C.-K.; Rosowski, F.; Trunschke, A.; Schlögl, R. The Microwave Cavity Perturbation Technique for Contact-Free and In-Situ Electrical Conductivity Measurements in Catalysis and Materials Science. *Phys. Chem. Chem. Phys.* **2012**, *14*, 1302–1312.